SUPPLEMENTARY INFORMATION

Differentiation stage determines reprogramming potential of hematopoietic cells into iPS cells

Sarah Eminli[*], Adlen Foudi[*], Matthias Stadtfeld, Nimet Maherali, Tim Ahfeldt, Gustavo Mostoslavsky, Hanno Hock, Konrad Hochedlinger

CONTENTS

1. Supplementary Figures 1-8
2. Supplementary Table 1

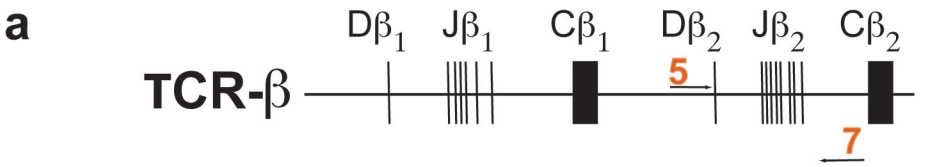

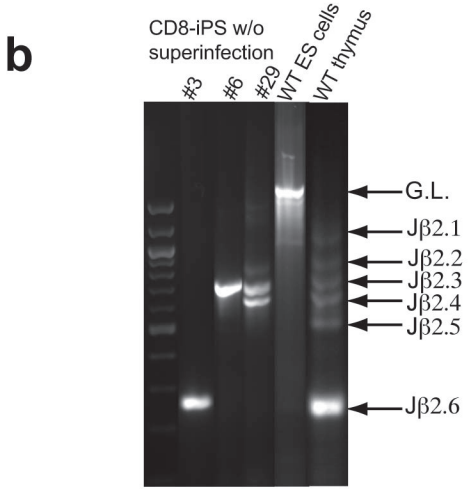

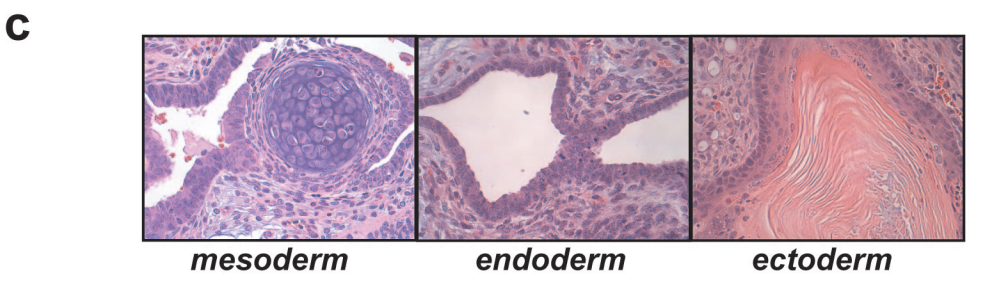

Supplementary Figure 1. Generation of iPS cells from fetal liver-derived CD8$^+$ T cells in the absence of superinfection. **(a)** Schematic of TCRβ locus showing primer binding sites (5,7) to detect Dβ2-Jβ2 rearrangements. **(b)** TCRβ D-J rearrangements by PCR on DNA isolated from three different CD8-iPS cell lines derived without lentiviral superinfection (compare Figure 3D, b), **(c)** Hematoxylin and eosin (H&E) staining of a representative teratoma section derived from such CD8-iPS cells shows pluripotency.

Supplementary Figure 1

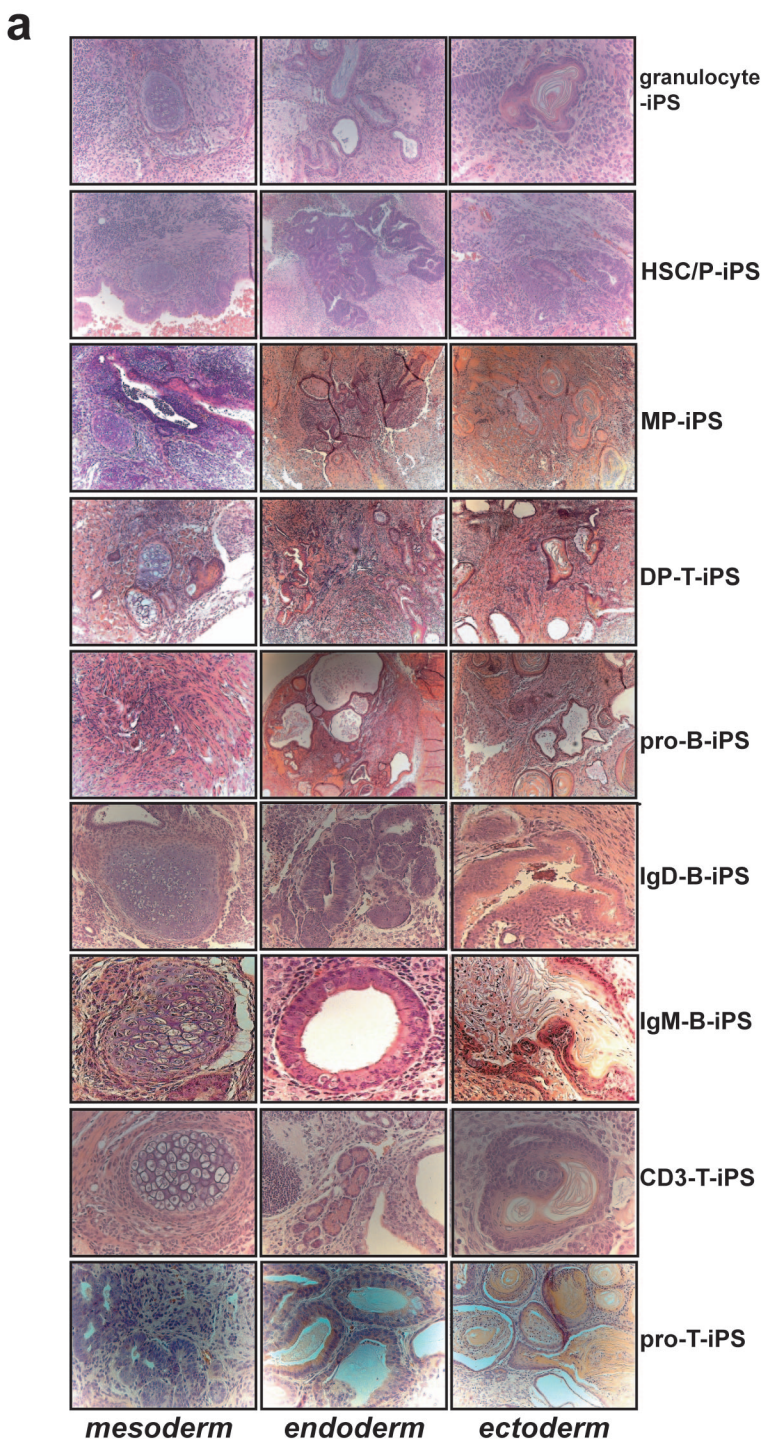

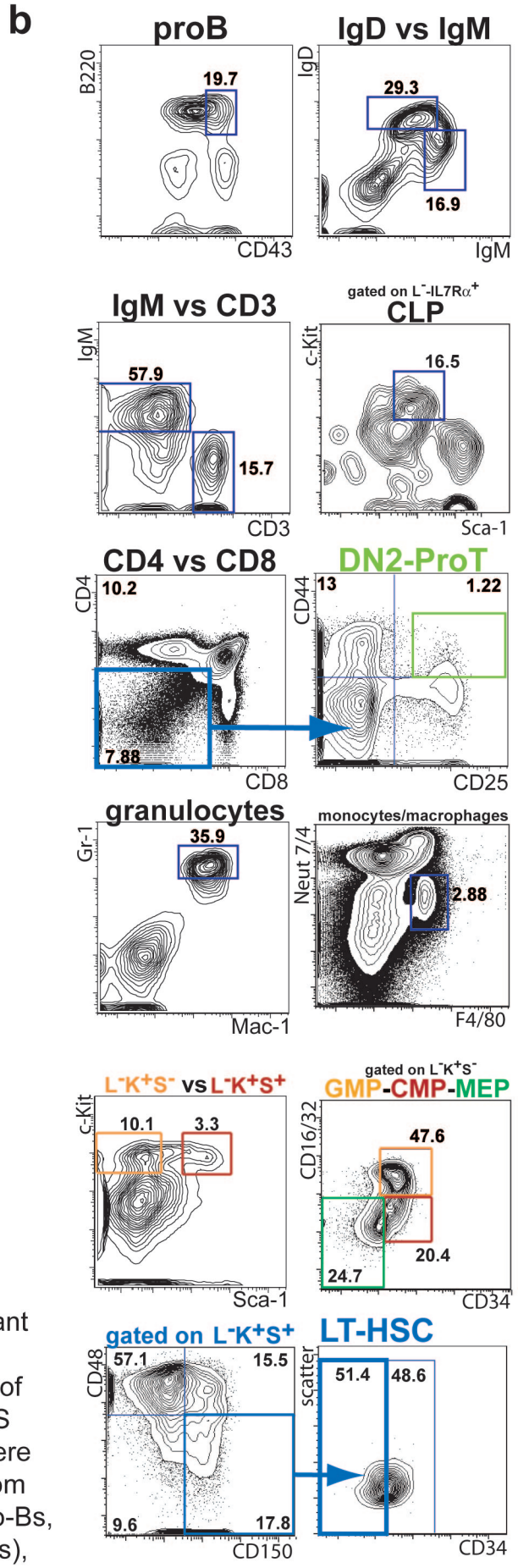

Supplementary Figure 2. Gating strategies for different hematopoietic cell types and differentiation potential of resultant iPS cell lines. **(a)** H&E staining of representative teratoma sections derived from iPS cells generated from different cells of the hematopoietic system. **(b)** Representative graphs of FACS plots indicate the gating strategies used in this study. Cells were stained as described in material and methods and isolated from BM (LT-HSCs, HSC/Ps, MPs, CLPs, CMPs, MEPs, GMPs pro-Bs, granulocytes and macrophages), spleen (mature B and T cells), lymph nodes (mature B cells, not shown) and thymus (immature T cell populations).

Supplementary Figure 2

a

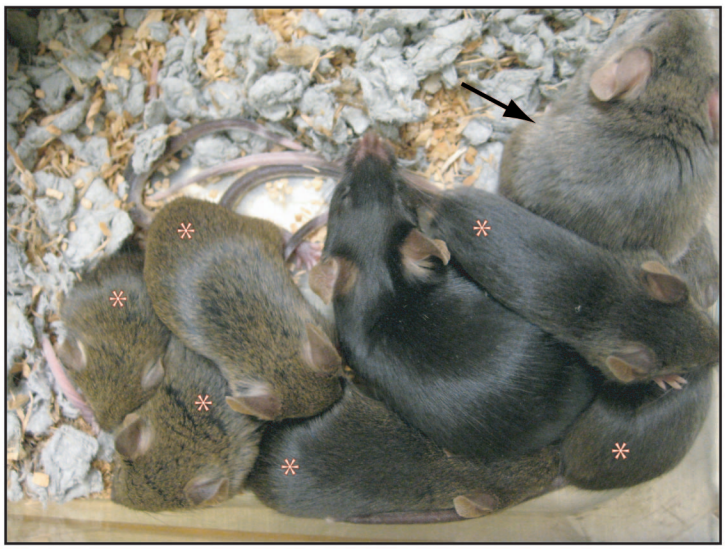

b

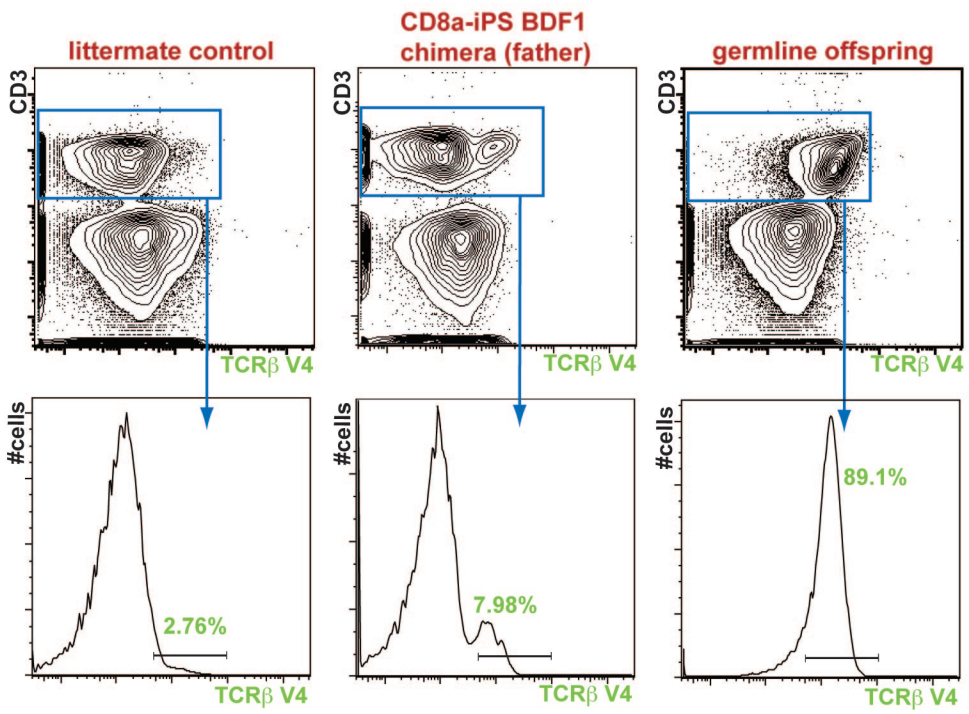

Supplementary Figure 3. Germline transmission of CD8-iPS chimeras. **(a)** Shown are a high-degree male chimera derived from CD8-iPS cells (arrow), a BDF1 female (black coat color) and their germline offspring (red asterisks). Note that all offspring are agouti-colored, indicating 100% germline transmission. **(b)** Molecular verification of germline transmission and monoclonality of lymphoid system. FACS plots to detect the functionally rearranged TCRβ alelle (Vβ4.1) in Vβ4.1-negative littermate control (left), CD8-iPS male chimera (center) and one Vβ4.1-positive germline offspring (right). Note the increased fraction of Vβ4.1-positive cells in the chimera and the monoclonal expression of Vβ4.1 in CD3+ T cells of one offspring.

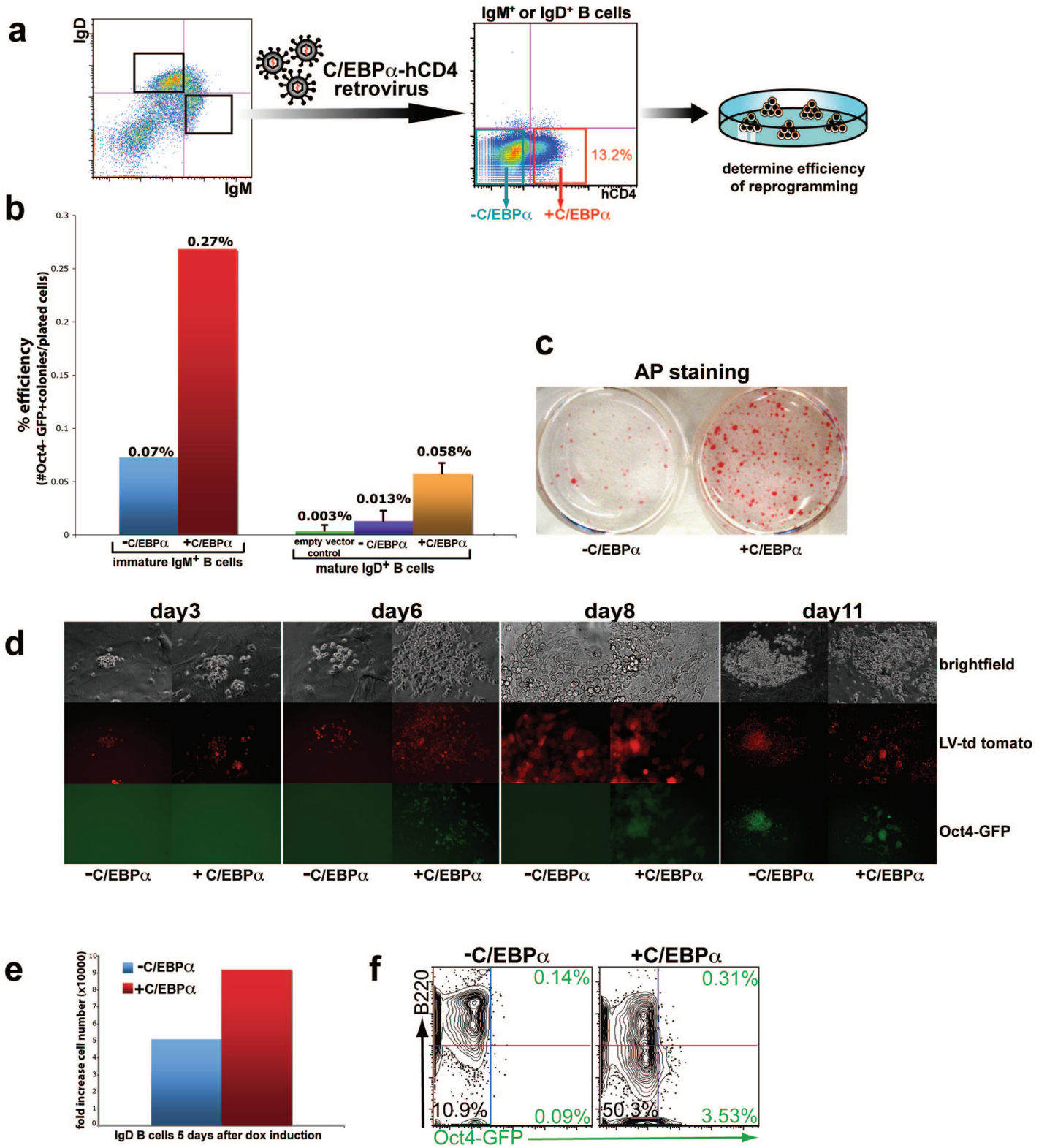

Supplementary Figure 4. Ectopic C/EBPα expression enhances basal reprogramming efficiency of B lymphocytes into iPS cells. (**a**) IgD$^+$ and IgM$^+$ splenocytes were isolated by FACS from adult CD8-iPS chimeras and infected with retrovirus encoding a C/EBPα-hCD4 cassette. (**b**) Number of Oct4-GFP+ iPS colonies derived from IgM$^+$ and IgD$^+$ B cells in the presence (+) or absence (-) of C/EBPα expressing virus. Note that there is a 5-to-20-fold increase in reprogramming efficiency of B lymphocytes expressing C/EBPα over uninfected cells or cells infected with an empty control virus. (**c**) Alkaline phosphatase (AP) staining of iPS colonies emerging from IgD cells in the presence of absence of C/EBPα-expressing virus. (**d**) C/EBPα-expressing B cells undergo faster reprogramming. Shown are images of emerging iPS colonies in the presence and absence of virus. Note the appearance of Oct4-GFP+ colonies by day 6 in C/EBPα-expressing cells compared with uninfected controls. (**e**) C/EBPα-expressing B cells proliferate more. Bars represent fold increase of the number of cells counted 5 days after doxycycline induction relative to the number plated at day 0 (not shown). (**f**) C/EBPα expression accelerates reprogramming of B cells. C/EBPα-expressing B cells downregulate the B cell marker B220 and activate Oct4-GFP sooner compared with uninfected controls at day 5 after dox induction.

Supplementary Figure 4

a

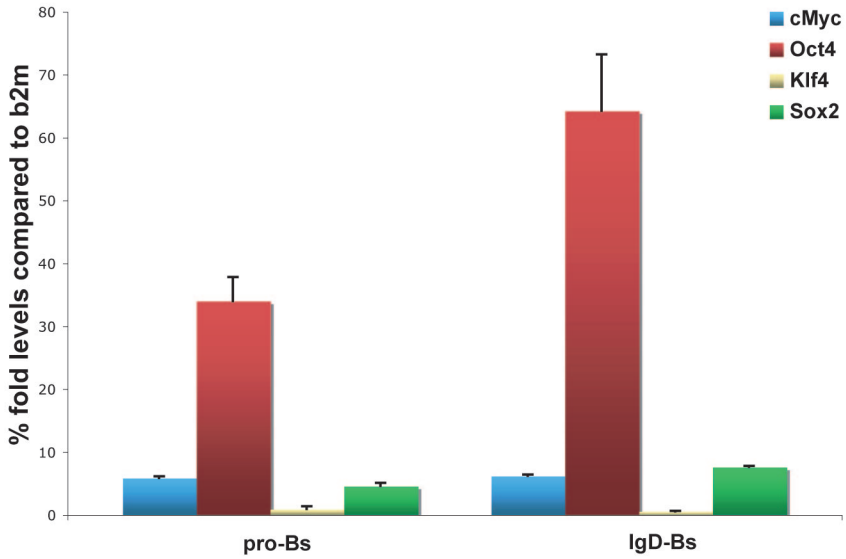

b

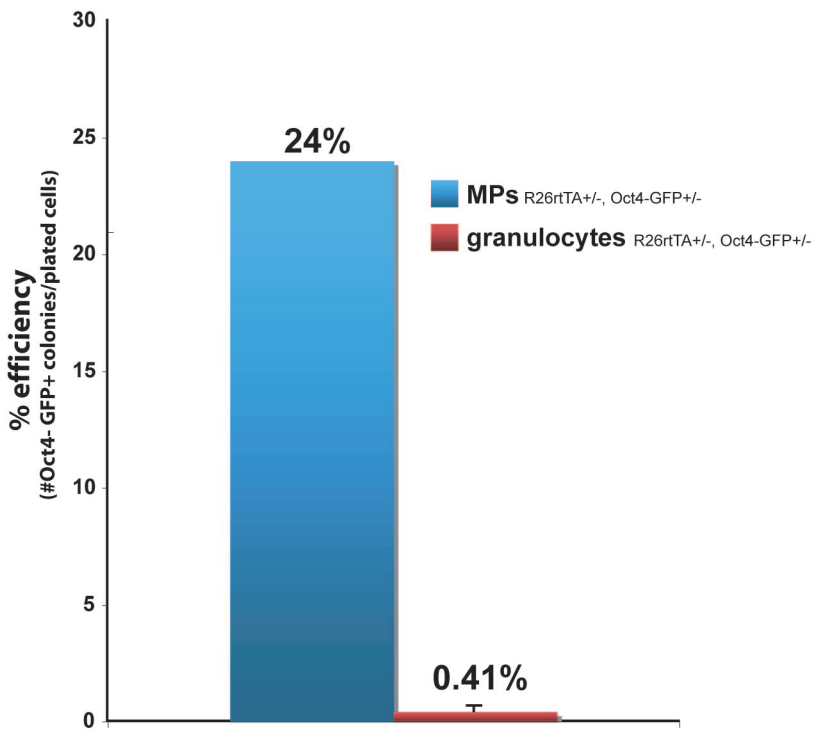

Supplementary Figure 5. Transgene expression in pro-B cells vs. B cells and reprogramming efficiencies of MPs and granulocytes upon direct viral infection. **(a)** Quantitative RT-PCR to detect viral transgene expression in chimera-derived pro-Bs and IgM^{low} IgD^{high} B cells treated with dox for 48h. Average expression levels and standard deviation from two different experiments (triplicate reactions) are shown for all four factors. **(b)** Efficiencies of iPS cell formation from MPs (5x10^4) and granulocytes (5x10^4) derived from a ROSA26-rtTA+/- Oct4-GFP+/- animal upon direct viral infection with a polycistronic lentivirus expressing Oct4, Sox2, Klf4 and cMyc. Reprogramming efficiencies were adjusted by measuring viral infection efficiencies with a GFP-expressing lentivirus.

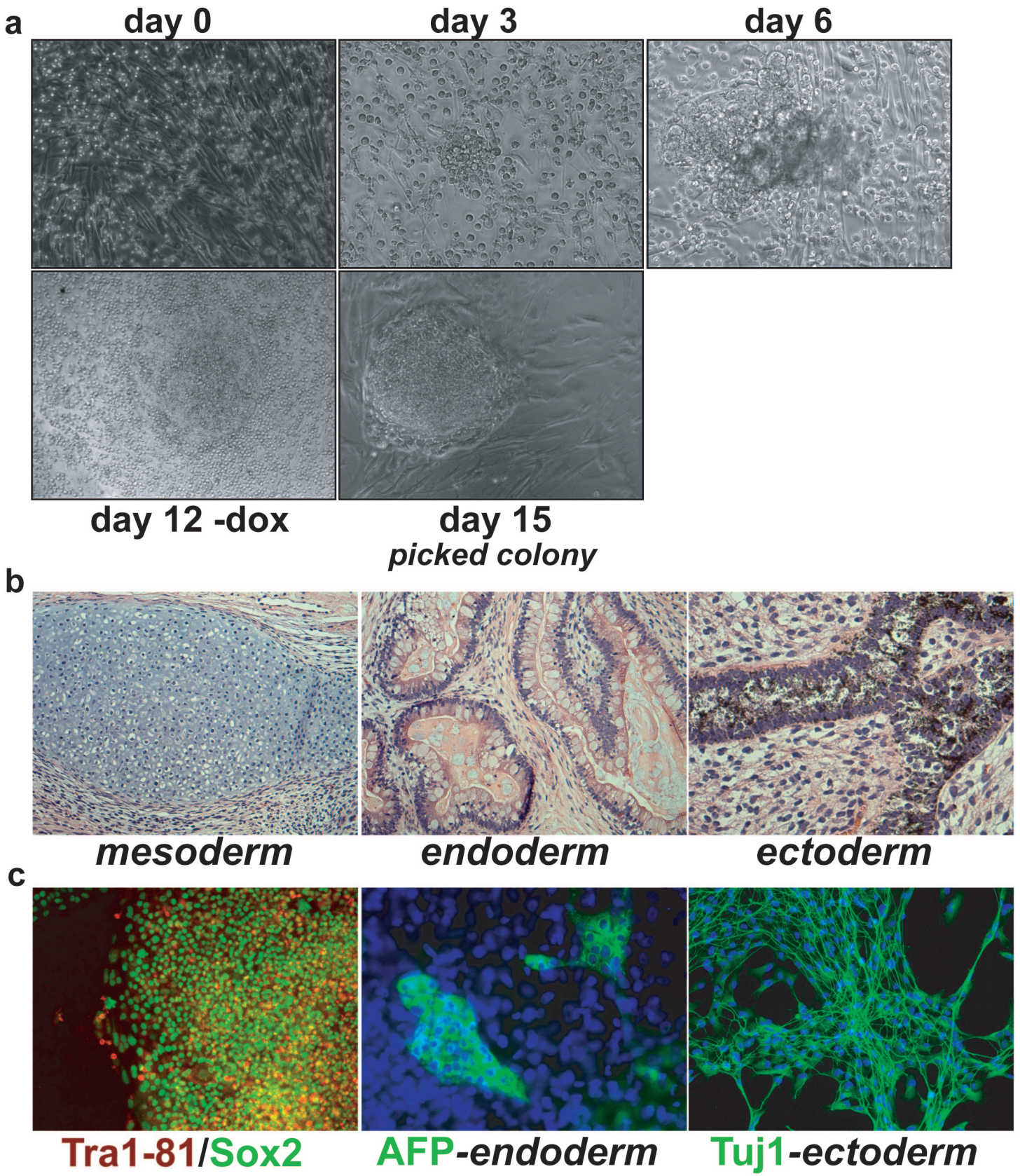

Supplementary Figure 6. Developmental potential of human CD34$^+$ cord blood cells. (**a**) Time course of morphological changes of human CD34$^+$ cord blood cells undergoing reprogramming. (**b**) H&E staining of representative teratoma sections from human CD34-iPS cells (mesoderm-cartilage, endoderm- gut-like epithilium/goblet-cells, ectoderm-melanocytes). (**c**) Immunostaing of pluripotency markers Tra1-81 (PE) and Sox2 (FITC), endoderm marker alpha-feto-protein (AFP-FITC) and ectoderm marker Neuron-specific class III β-tubulin (Tuj1-FITC). Nuclei are shown in DAPI (blue).

Supplementary Figure 6

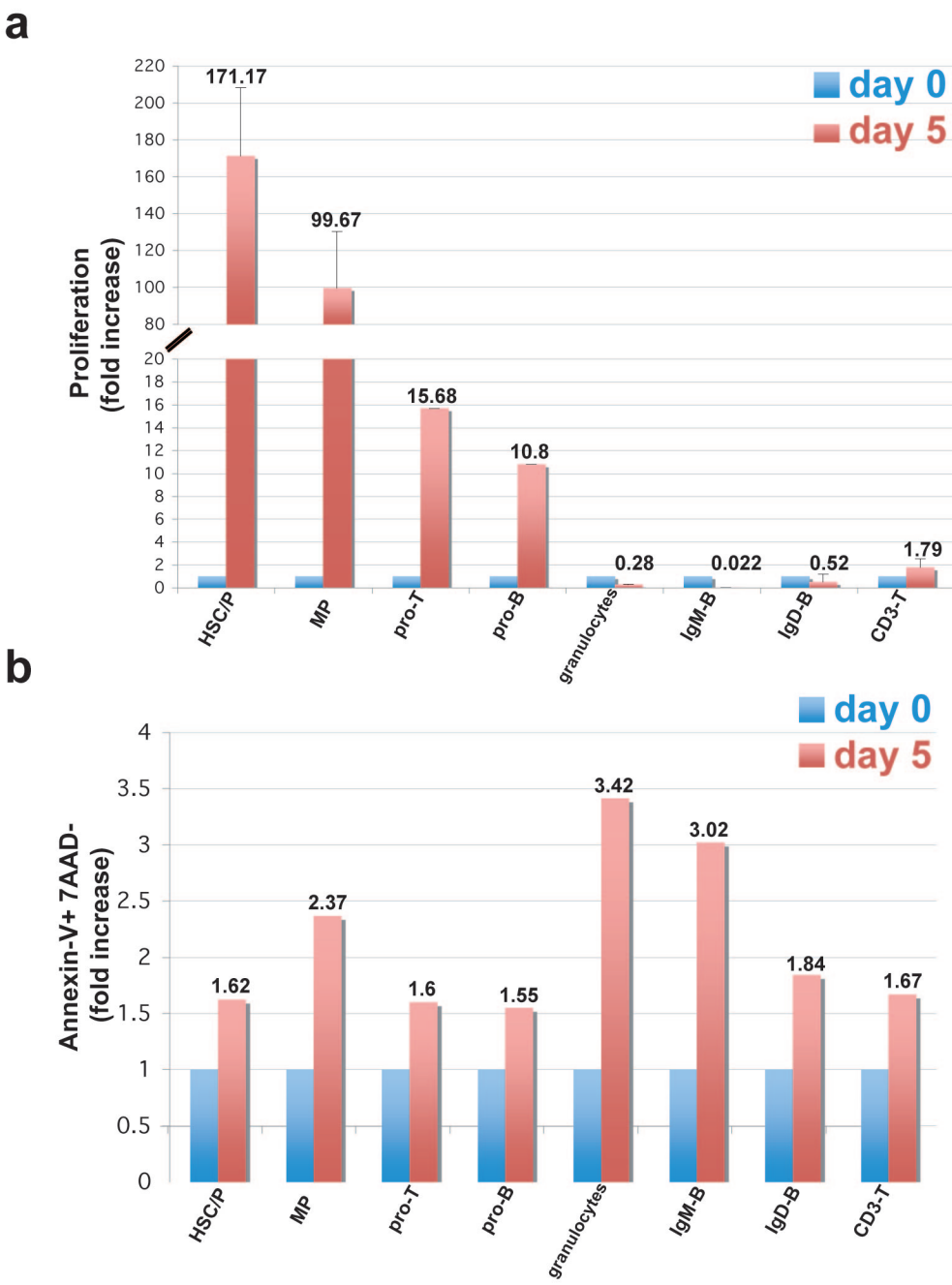

Supplementary Figure 7. Measurement of proliferation and apoptosis in immature and mature blood cell types.(**a-b**) iPS-derived hematopoietic cells were isolated by FACS and cultured *in vitro* as described in materials and methods. 5x10^3 to 2x10^6 cells were plated at day 0 and cultured under normal growth conditions in the presence of cytokines. (**a**) After 5 days, trypan blue negative cells were counted using a hemacytometer. Bars represent fold increase or decrease of the number of cells counted 5 days later (red bars) relative to the number plated at day 0 (blue bars). (**b**) Apoptosis assay was performed on day 0 and day 5 in these cultures, as described in materials and methods. Bars represent the fold increase of the percentage of Annexin-V+7-AAD- apoptotic cells (dead cells excluded) observed at day 5 (red bars) relative to day 0 (blue bars). Bars represent mean ± SD. Numbers above each bar represents the mean value for that sample.

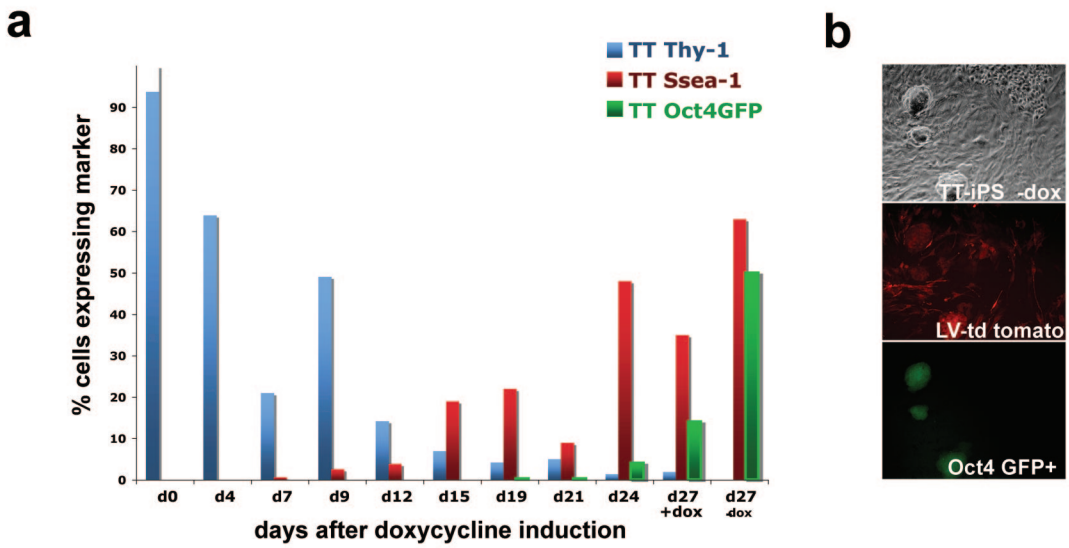

Supplementary Figure 8. Reprogramming kinetics of tail fibroblasts from CD8-iPS chimeras. (**a**) Time course of Thy-1 and SSEA-1 surface marker expression and Oct4-GFP activity in tdTomato positive sorted tail-tips (TT) fibroblasts derived from CD8-iPS chimera undergoing reprogramming as determined by FACS. (**b**) ES cell morphology of tdTomato- and Oct4-GFP expressing iPS cells derived from TT fibroblasts at day 27, following discontinuation of doxycycline treatment.

RT-PCR primer 5'-3' sequence	
3' tetO-myc	AAGAGGACTTGTTGCGGAAA
5' tetO-myc	TTGTAATCCAGAGGTTGATTATCG
3' tetO-Klf4	ATGGTCAAGTTCCCAGCAAG
5' tetO-Klf4	TGATATCGAATTCCGTTTGTTT
3' tetO-Oct4	AGTTGGCGTGGAGACTTTGC
5' tetO-Oct4	CAGGGCTTTCATGTCCTGG
3' tetO-Sox2	GGCCATTAACGGCACACT
5' tetO-Sox2	AAGCAGCGTATCCACATAGC
3' b2m	TTCTGGTGCTTGTCTCACTGA
5' b2m	CAGTATGTTCGGCTTCCCATTC

Supplementary Table 1. Real-time quantitative PCR primer sequences.